J Mater Sci (2011) 46:6883–6888
DOI 10.1007/s10853-011-5652-z

Fabrication of polypyrrole/layered niobate nanocomposite and its electrochemical behavior

Juanjuan Ma · Heng Jiang · Ningze Zhuo · Jingfei Li · Jiawei Lu · Junyan Gong · Xingyou Xu · Zhiwei Tong

Received: 28 March 2011 / Accepted: 21 May 2011 / Published online: 2 June 2011

Abstract Polypyrrole/layered niobate (PPy–Nb_6O_{17}) nanocomposite has been synthesized by the intercalation of pyrrole monomer into the layer structure of organo-modified niobate followed by the subsequent in situ polymerization of pyrrole in the interlayer spaces. The microstructure and morphology characterizations for the resulting material have been investigated by means of XRD, FTIR, and SEM. On the basis of the experimental results, the mechanism for the formation of PPy chains within the confined galleries of the inorganic host material is presented. The cyclic voltammogram of the PPy–Nb_6O_{17} nanocomposite thin film exhibits a fine diffusion-controlled electrode process, which hints the possibility of being utilized as an electrode modifying material.

Introduction

Layered nanocomposites fabricated by the intercalation of guest species into the two-dimensional (2D) host interlayer regions have attracted considerable attention [1]. Among the diverse host materials, a series of layered compounds based on niobates and titanates such as $K_4Nb_6O_{17}$, KNb_3O_8, $KTiNbO_5$, KTi_2NbO_7, and $KCa_2Nb_3O_{10}$ are attractive host materials due to high ion exchangeability and unique structural properties. Intercalation compounds derived from these layered transition metal oxides have been extensively investigated for potential applications in various aspects, such as photocatalysis [2, 3], electrochemical electrode [4], photoinduced electron transfer [5, 6], etc.

On the other hand, polyaniline (PAni) and polypyrrole (PPy) are the most studied conducting polymers. In recent years, composites of conducting polymers and layered inorganic solids have exhibited great promise due to their conductivity, high thermal stability, and high charge capacity [7–10]. Among these studies, several groups have successfully incorporated polyaniline in layered niobates and titanates [11–14]. In a typical synthetic procedure, aniline monomer was introduced into the 2D galleries by neutralization with protonated oxides, followed by in situ intercalative polymerization. To the best of our knowledge, however, no examples of the synthesis of PPy/layered niobate nanocomposite have been reported so far.

Unlike aniline, pyrrole is acidic, so it cannot be intercalated by acid–base reaction or cation exchange. Letaïef et al. [15] have successfully prepared PPy–clay nanocomposites by adsorption of pyrrole vapor and the intercalative polymerization. Bissessur et al. [16] have shown that PPy can be directly inserted into MoS_2 by making use of the exfoliating and restacking properties of $LiMoS_2$. Yoshimoto et al. [17] applied the mechanochemical technique to incorporate PPy chains into clay galleries. Herein, $K_4Nb_6O_{17}$ is organically modified with a cationic surfactant octadecyl trimethyl ammonium chloride (OTAC)

J. Ma · H. Jiang · N. Zhuo · J. Li · J. Lu · J. Gong · Z. Tong (✉)
Department of Chemical Engineering, Huaihai Institute of Technology, Lianyungang 222005, China
e-mail: zhiweitong575@hotmail.com

J. Ma · X. Xu
Key Laboratory of Soft Chemistry and Functional Materials, Ministry of Education, Nanjing University of Science and Technology, Nanjing 210094, China

X. Xu
School of Life Science and Chemical Engineering, Huaiyin Institute of Technology, Huaian 223003, China

Z. Tong
SORST, Japan Science and Technology (JST), Tsukuba, Japan

before the intercalation of the pyrrole monomer. With the addition of initiator, PPy is formed by in situ polymerization in the organophilic gallery. The obtained PPy–Nb_6O_{17} hybrid is characterized by X-ray diffraction (XRD), infrared spectra (IR), and scanning electron microscopy (SEM). Based on the experimental data, the mechanism for the formation of PPy chains in the interlayer region of niobate has been proposed. Electrochemical studies indicate that the glass carbon electrode (GCE) modified with the as-prepared PPy–Nb_6O_{17} hybrid exhibits good redox activity and electrochemical-cycling stability.

Experimental

Materials

A layered compound $K_4Nb_6O_{17}\cdot 3H_2O$ was synthesized by calcination of a 2.1:3.0 molar mixture of K_2CO_3 and Nb_2O_5 at 1100 °C for 10 h, according to the procedure described in the literature [18]. Pyrrole was purified by distillation under reduced pressure prior to use. The other materials were purchased as analytical grade chemicals.

Preparation of PPy–Nb_6O_{17} nanocomposite

The suspension of layered niobate $K_4Nb_6O_{17}$ was first treated with aqueous solution of OTAC for 3 weeks at room temperature. The molar ratio of OTAC to $K_4Nb_6O_{17}$ was 8:1. The product was washed with water until the washing became Cl^- free and then was dried under ambient conditions. The organo-modified niobate (OTAC–Nb_6O_{17}) was then allowed to react with a pyrrole methanol/water solution (1/2, v/v) under N_2 atmosphere for another 2 weeks at room temperature. The product was filtered, washed with methanol until pyrrole could not be detected at 246 nm by UV spectroscopy in the filtrate and termed as Py–Nb_6O_{17}. Polymerization was carried out by the dropwise addition of 0.2 M aqueous solution of $FeCl_3$ ($FeCl_3$/pyrrole molar ratio 2/1) to the Py–Nb_6O_{17} suspension and continued for 24 h with stirring at room temperature. Then the reaction mixture was filtered and washed with copious water until free of Cl^-. Finally the obtained gray powder was dried in vacuum at 40 °C overnight and termed as PPy–Nb_6O_{17}. Reference PPy sample was prepared under the same condition using $FeCl_3$ as oxidant in OTAC aqueous solution.

Characterization

X-ray diffraction patterns were obtained with a RINT 2000 diffractometer (Rigaku), using Cu Kα radiation ($\lambda = 0.154$ nm) with 2θ from 1.5° to 20°. Data were collected at a scanning rate of 1.0° min^{-1}. The infrared spectrum was recorded on a Shimadzu FTIR-8400S spectrometer with the use of KBr pellets. Scanning electron micrograph images were taken with a JSM-5600 apparatus (JEOL) operating at 15 kV for the Au-coated samples. The elemental analysis was performed using a Perkin Elmer 2400-CHN elemental analyzer.

Electrochemical measurements were performed with a three-electrode electrochemical cell, with a platinum wire being used as the counter electrode, and a saturated calomel electrode as the reference electrode. The glassy carbon electrode (GCE, area 0.38 cm^2) was hand polished directly with slurry of 1.0 and then 0.3 μm alumina and used as the working electrode. The PPy–Nb_6O_{17} nanocomposite and reference PPy films were deposited onto the GCE.

Results and discussion

Synthesis of PPy–Nb_6O_{17} nanocomposite

To confirm the intercalation of PPy into the interlayer spaces of organo-modified niobate, various kinds of characterization have been applied. Figure 1 presents the XRD patterns of $K_4Nb_6O_{17}\cdot 3H_2O$ as starting material (a), after organo-modification (b), after intercalation in the presence of pyrrole (Py–Nb_6O_{17}) and after in situ polymerization (PPy–Nb_6O_{17}) (d). The hydrated potassium niobate, $K_4Nb_6O_{17}\cdot 3H_2O$, exhibits a (020) diffraction peak at 1.88 nm accompanied by an intense (040) peak at 0.94 nm. There exist two types of interlayers (hydrated interlyers I and non-hydrated interlayers II) alternately (Fig. 2). The ion exchangeability of the adjacent two interlayers is different from each other [19, 20]. The d_{020} value corresponds to the sum of two adjacent interlayer spaces. In the XRD pattern of OTAC–Nb_6O_{17}, the (020) peak disappears and the (040)

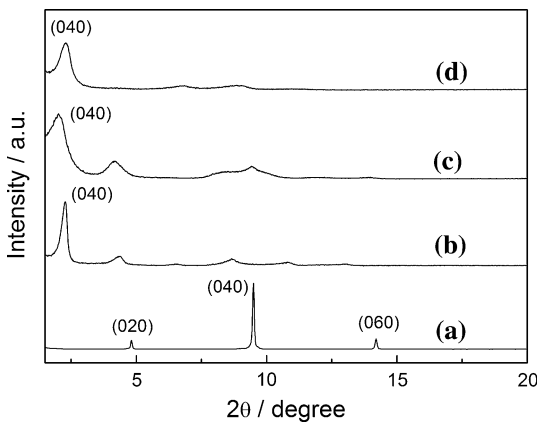

Fig. 1 X-ray diffraction patterns of (*a*) $K_4Nb_6O_{17}\cdot 3H_2O$, (*b*) OTAC–Nb_6O_{17}, (*c*) Py–Nb_6O_{17}, and (*d*) PPy–Nb_6O_{17}

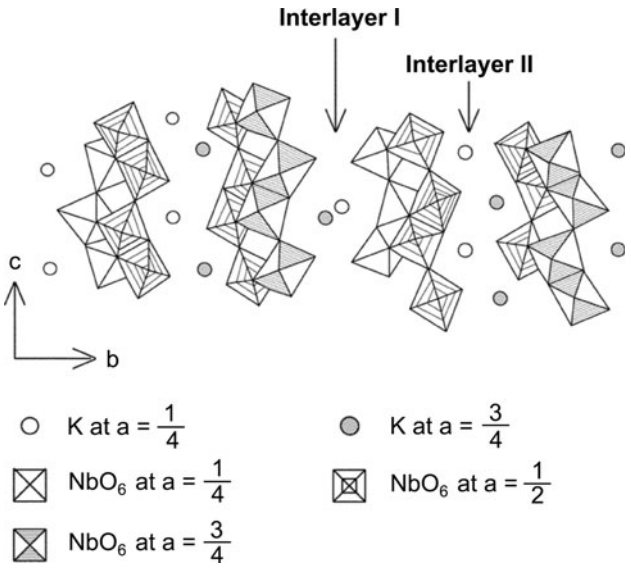

Fig. 2 Schematic structure of $K_4Nb_6O_{17}$

peak appears at 3.87 nm. These observations indicate that OTAC molecules can be inserted not only into interlayer I, but also into interlayler II. By subtracting the thickness of niobate slab (0.41 nm), the net interlayer height of OTAC–Nb_6O_{17} is 3.46 nm. Considering the size of OTAC chain length (2.6 nm, estimated by Chem 3D for an optimized structure by PM3 calculation), it is postulated here that OTAC cations may form a double layer in the interlayer region and the tilt angle of OTAC is estimated to be 42° with respect to the niobate nanosheet [21]. The intercalation of bulky ions into the interlayer spaces is difficult owing to the high charge densities of niobate layers. Herein, a long time of 3 weeks are needed for OTAC cations to enter into both interlayer I and interlayer II. [22, 23] After the loading of pyrrole monomer, the (040) diffraction peak of the product shifts to a lower angle compared to OTAC–Nb_6O_{17}, indicating the successful insertion of pyrrole into the lamellar spaces. The basal spacing of Py–Nb_6O_{17} reaches 4.37 nm. The driving force for intercalation of non-ionic pyrrole molecules into organically modified niobate is assumed to be hydrophobic interactions with the intercalated alkyl chains of OTAC–Nb_6O_{17} and the formation of hydrogen bonding interactions between the N–H of the pyrrole and the surface oxygen atoms of the niobate. The layer distance begins to shrink as the in situ polymerization progressed. The basal spacing of 3.84 nm is close to that of OTAC–Nb_6O_{17} before the intercalation of pyrrole. The decrease in the basal spacings could be due to the chemical bonding of monomers during the polymerization and the partial expulsion of the pyrrole molecules from the interlayer spaces. Similar results were also observed in the intercalative polymerization of aniline and pyrrole within other various layered hosts [12, 17].

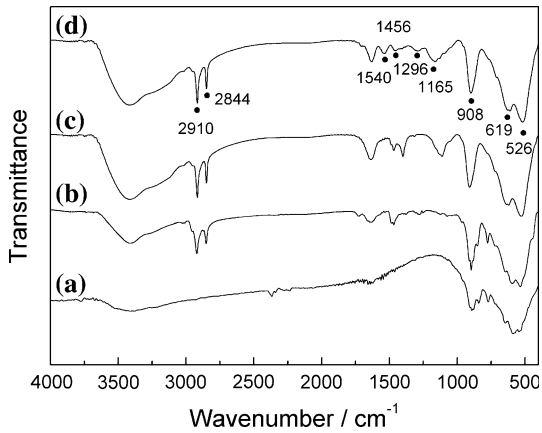

Fig. 3 IR spectra of (*a*) $K_4Nb_6O_{17}\cdot 3H_2O$, (*b*) OTAC–Nb_6O_{17}, (*c*) Py–Nb_6O_{17}, and (*d*) PPy–Nb_6O_{17}

To further prove PPy chains have been intercalated into the niobate galleries, FTIR spectrum was measured for the resulting product after polymerization, as shown in Fig. 3. For comparison, the IR spectra of pristine unmodified $K_4Nb_6O_{17}$, organically modified OTAC–Nb_6O_{17} and Py–Nb_6O_{17} are also presented. In the FTIR spectrum of PPy–Nb_6O_{17} hybrid, the absorption bands at 1540, 1456, 1296, and 1165 cm^{-1} are ascribed to the PPy chain [24, 25]. The peak at 1540 cm^{-1} is associated with the pyrrole ring, i.e., the combination of C=C and C–C stretching vibrations. The peak at 1456 cm^{-1} is due to the C–N stretching vibration. The peaks at 1296 and 1165 cm^{-1} are attributed to the in-plain vibrations of C–H. Furthermore, C–H antisymmetric and symmetric stretch vibrations appear at 2910 and 2844 cm^{-1}, corresponding to hydrocarbon chains of OTAC molecules in the hybrid. The absorption bands in the range of 400–1000 cm^{-1} arise from the Nb–O stretching vibration of the layered host [26]. The IR absorption of PPy–Nb_6O_{17} hybrid is different from that of Py–Nb_6O_{17} in the range of 1000–1650 cm^{-1}, which is caused by the chemical bonding between pyrrole rings in polymer chains. Above spectral results confirm that the intercalative polymerization of pyrrole within the niobate nanosheets is successfully carried out to produce PPy–Nb_6O_{17} hybrid.

The SEM images of $K_4Nb_6O_{17}\cdot 3H_2O$ and PPy–Nb_6O_{17} hybrid are given in Fig. 4. The SEM image of $K_4Nb_6O_{17}\cdot 3H_2O$ shows 2D niobate sheets in a parallel layered structure. The intercalation of polymer does not disturb the lamellar structure of the niobate. Furthermore, CHN analysis of PPy–Nb_6O_{17} hybrid reveals that the C/N molar ratio is 16.6. This value is between that of OTAC and polypyrrole, which further confirm the coexistence of OTAC and polypyrrole in the hybrid. According to the above experimental results, the proposed mechanism for the formation of PPy–Nb_6O_{17} nanocomposite is shown in

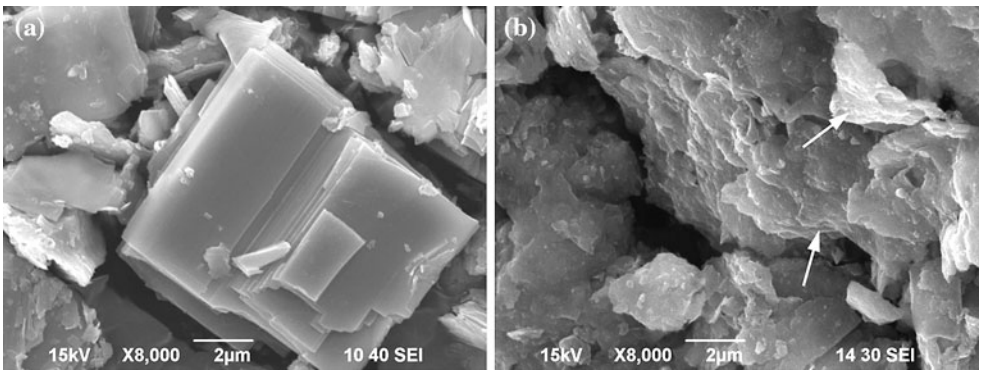

Fig. 4 SEM micrographs of **a** $K_4Nb_6O_{17}{\cdot}3H_2O$ and **b** PPy–Nb_6O_{17}

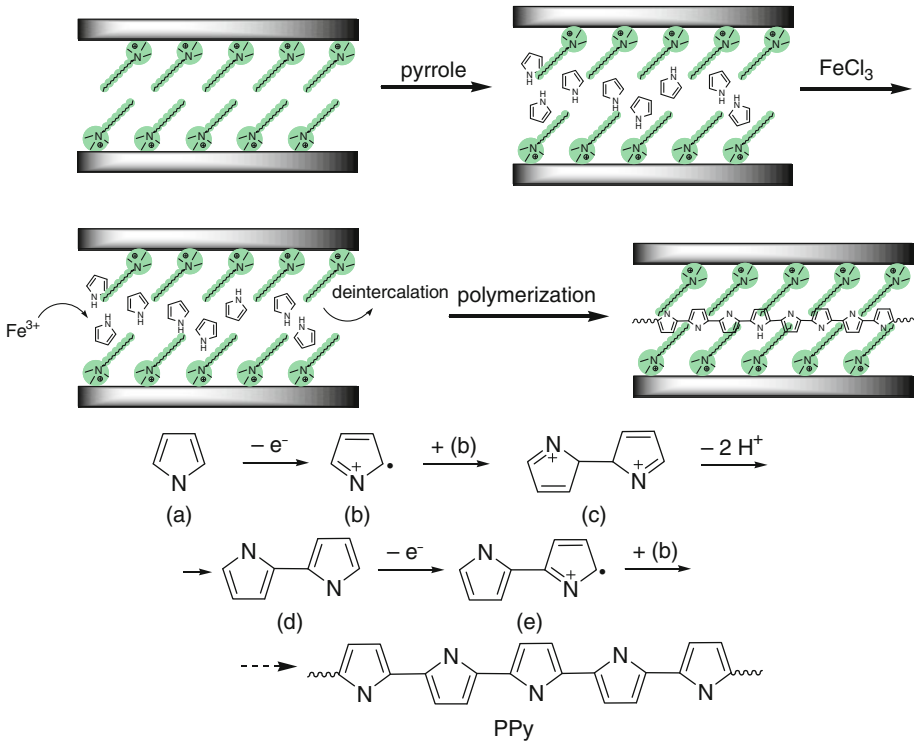

Fig. 5 Proposed mechanism for the intercalation and polymerization of pyrrole between the niobate layers

Fig. 5 [27]. When Fe^{3+} ions move into the interlayer spaces, they are able to oxidize the intercalated monomers yielding highly active intermediate species, cation radicals, thus initiating the polymerization process. Once formed, cation radicals react with monomer molecules, yielding dimers, oligomers, and polymers as end product of oxidative polymerization.

Electrochemical properties of the PPy–Nb_6O_{17} modified electrode

Cyclic voltammograms, obtained with the GCE modified only with $K_4Nb_6O_{17}{\cdot}3H_2O$ in 0.1 M $LiClO_4$ solution, reveals no peak in the potential range of −1.2–1.2 V (Fig. 6a) in either scan directions. However, when PPy is intercalated into the interlayer spaces of layered niobate, clear cyclic voltammetric waves are observed with anodic and cathodic peak currents at −0.65 and −0.87 V, respectively (Fig. 6c). This pair of peaks is attributed to the involvement of the redox couple [PPy^+, ClO_4^-]/PPy. During the anodic sweep, PPy gets oxidized resulting in production of positive sites in the originally neutral matrix [28]. In order to maintain the electroneutrality of the polymer, ClO_4^- ions migrate into the matrix from the electrolyte during the anodic sweep and are expelled during the cathodic sweep. The midpoint potential [$E_m = (E_{pa} + E_{pc})/2$] and the peak separation ($\Delta E_p = E_{pa} - E_{pc}$) are found to be −0.76 and 0.22 V, respectively. For comparison, the cyclic voltammogram of reference PPy is given in Fig. 6b, which presents one pair of broad redox

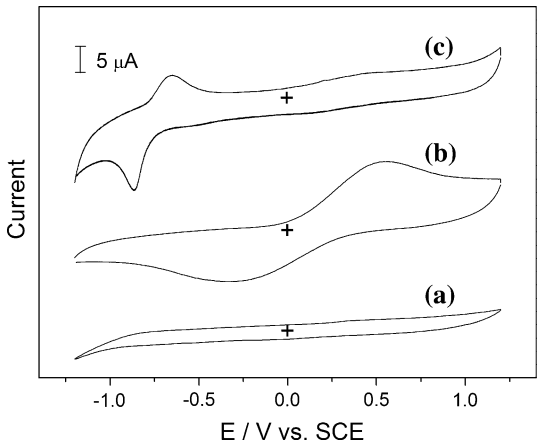

Fig. 6 Cyclic voltammograms of (*a*) $K_4Nb_6O_{17}{\cdot}3H_2O$, (*b*) Reference PPy and (*c*) PPy–Nb_6O_{17} modified electrodes in 0.1 M $LiClO_4$ solution under N_2 at a scan rate of 100 mV s^{-1}

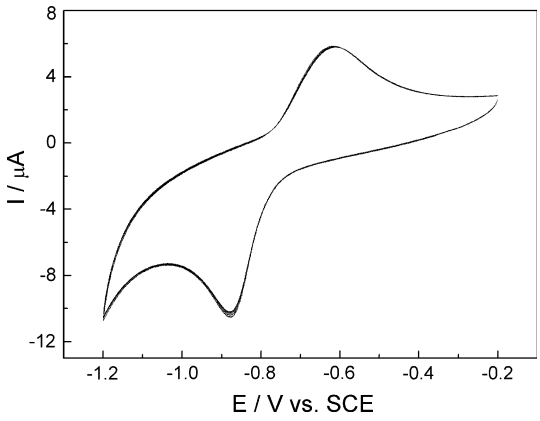

Fig. 8 Cyclic voltammograms upon repeated potential scans of PPy–Nb_6O_{17} hybrid thin film in 0.1 M $LiClO_4$ solution under N_2 at a scan rate of 100 mV s^{-1}

peak with a midpoint potential at $E_m = 0.125$ V and the peak separation $\Delta E_p = 0.69$. The difference in the electrochemical behaviors between the PPy–Nb_6O_{17} nanocomposite and reference PPy may originate from the fact that the layered host provides a nanometer-sized 2D channel for the polymerization of the PPy chains and for the transportation of conductive carrier during the redox process. For example, the introduction of niobate has varied a packed configuration of PPy to a looser one of PPy–Nb_6O_{17}, which can be used to explain the smaller peak separation in the voltammogram of PPy–Nb_6O_{17} [29].

Figure 7 illustrates the cyclic voltammograms of PPy–Nb_6O_{17} measured at different scan rates. There is a shift of E_{pc} to more negative values and a shift of E_{pa} to more positive values with the increase of the scan rate. The ΔE_p increases from 0.103 to 0.445 V when the scan rate varies

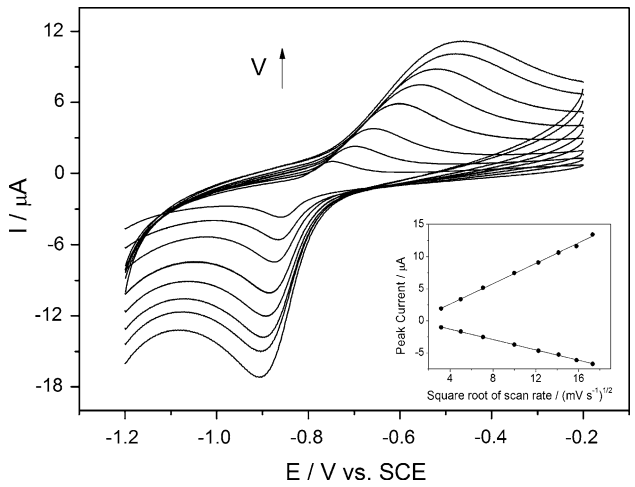

Fig. 7 Cyclic voltammograms of PPy–Nb_6O_{17} thin film in 0.1 M $LiClO_4$ solution under N_2 at a scan rate of 10, 25, 50, 100, 150, 200, 250, and 300 mV s^{-1}, respectively. *Inset* shows the relationship between peak current and square root of scan rate

from 10 to 300 mV s^{-1}, indicating a slow electron diffusion process of the PPy in the interlayer region at high scan rates. Plotting the cathodic and anodic peak currents (I_c and I_a) against the square root of the scan rate (inset), a linear correlation was obtained, suggesting a diffusion-controlled electrode process. This behavior may be explained due to the incorporation/expulsion of the ClO_4^- ions at the solid/solution interface during the redox process.

The stability of the obtained PPy–Nb_6O_{17} nanocomposite is a key aspect for its practical application. In order to verify the electrochemical stability of the PPy–Nb_6O_{17} hybrid film, the modified GCE is tested for repeated circles at the scan rate of 100 mV s^{-1}. It can be seen from Fig. 8 that the PPy–Nb_6O_{17} hybrid is very stable in $LiClO_4$ medium, with almost no observable changes in both the peak current and the peak separation after the first cycle, which confirms the good immobilization of PPy in niobate interlayer spaces. The results obtained from CVs reveal excellent redox activity and electrochemical stability of the nanocomposite, which indicate that PPy–Nb_6O_{17} is an attractive candidate for practical utilization as electronic conductors and catalysts in electronic devices with potential applications in sensors, batteries, optical switching devices, and so on.

Conclusions

The intercalation of pyrrole into the layered niobate semiconductor and the subsequent in situ polymerization of pyrrole are performed to develop a novel organic/inorganic hybrid material with interesting characteristics. The cationic surfactant molecules OTAC are introduced into the interlayer spaces to provide a strong driving force for the intercalation of pyrrole monomer. The intercalation process has been investigated systematically by several techniques,

including XRD, IR, and SEM. The electrochemical behavior of the nanocomposite modified electrode investigated by cyclic voltammetry exhibits a diffusion-controlled process and the excellent stability of the nanocomposite film has also been proved. We predict that PPy–Nb_6O_{17} nanocomposite has possibility to be used as electrode modifying material.

Acknowledgements This work was supported by National Natural Science Foundation of China (Grant No. 50873042, 21001048) and the Scientific Research Program of the HuaiHai Institute of Technology (Z2009021). The authors are also grateful to the Jiangsu Marine Resource Development Research Institute Foundation (JSIMR10E06).

References

1. Ogawa M, Kuroda K (1995) Chem Rev 95:399
2. Furube A, Shiozawa T, Ishikawa A, Wada A, Domen K, Hirose C (2002) J Phys Chem B 106:3065
3. Kiba S, Haga J, Hashimoto S, Nakato T (2010) J Nanosci Nanotechnol 10:8341
4. Zhang XB, Liu C, Liu L, Zhang DE, Zhang TL, Xu XY, Tong ZW (2010) J Mater Sci 45:1604. doi:10.1007/s10853-009-4134-z
5. Tong ZW, Shichi T, Takagi K (2002) J Phys Chem B 106:13306
6. Unal U, Matsumoto Y, Tamoto N, Koinuma M, Machida M, Izawa K (2006) J Solid State Chem 179:33
7. Kim BH, Jung JH, Hong SH, Joo J, Epstein AJ, Mizoguchi K, Kim JW, Choi HJ (2002) Macromolecules 35:1419
8. Boukerma K, Piquemal JY, Chehimi MM, Mravcakova M, Omastova M, Beaunier P (2006) Polymer 47:569
9. Yoshimoto S, Ohashi F, Ohnishi Y, Nonami T (2004) Synth Met 145:265
10. Huguenin F, Ticianelli EA, Torresi RM (2002) Electrochim Acta 47:3179
11. Inui Y, Yui T, Itoh T, Higuchi K, Seki T, Takagi K (2007) J Phys Chem B 111:12162
12. Yang G, Hou WH, Feng XM, Xu L, Liu YG, Wang G, Ding WP (2007) Adv Funct Mater 17:401
13. Ma JJ, Zhang XB, Yan C, Tong ZW, Inoue HR (2008) J Mater Sci 43:5534. doi:10.1007/s10853-008-2837-1
14. Liu C, Zhan XB, Wang S, Liu L, Guo LC, Tong ZW, Inoue HR (2010) Chem Lett 39:122
15. Letaïef S, Aranda P, Ruiz-Hitzky E (2005) Appl Clay Sci 28:183
16. Bissessur R, Liu PKY (2006) Solid State Ion 177:191
17. Yoshimoto S, Ohashi F, Kameyama T (2005) Macromol Rapid Commun 26:461
18. Nassau K, Shiever JW, Bernstei JL (1969) J Electrochem Soc 116:348
19. Nakato T, Sakamoto D, Kuroda K, Kato C (1992) Bull Chem Soc Jpn 65:322
20. Kinomura N, Kumada N, Muto F (1985) J Chem Soc Dalton Trans 2349
21. Yamaguchi Y, Yui T, Takagi S, Shimada T, Inoue H (2001) Chem Lett 30:644
22. Nakato T, Kameyama M, Wei QM, Haga J (2008) Microporous Mesoporous Mater 110:223
23. Tang YM, Nian JQ, Yu B, Yang WZ (2009) Mater Lett 63:1992
24. Liu J, Wan M (2001) J Mater Chem 11:404
25. Wang T, Liu W, Tian J, Shao X, Sun D (2004) Polym Compos 25:111
26. Jehng JM, Wachs IE (1991) Chem Mater 3:100
27. Malinauskas A (2001) Polymer 42:3957
28. Singh RN, Malviya M, Anindita, Sinha ASK, Chartier P (2007) Electrochim Acta 52:4264
29. Ding KQ, Cheng FM (2009) Synth Met 159:2122